ISSN (Online): 2455-3662
EPRA International Journal of Multidisciplinary Research (IJMR) - Peer Reviewed Journal
Volume: 10| Issue: 3| March 2024|| Journal DOI: 10.36713/epra2013 || SJIF Impact Factor 2024: 8.402 || ISI Value: 1.188

TUNNING OF PHOTOCATALYTIC PERFORMANCE OF CrO_4-ZrO_2 NANOCOMPOSITE MATERIAL FOR THE EFFECTIVE DEGRADATION OF INDUSTRIAL DYES

K. Subashri
Ph.D Research Scholar, Department of Chemistry, Centre for Research and Evaluation, Bharathiar University, Coimbatore 641046, Tamilnadu, India.

ABSTRACT
Revolutionary nanocomposite material of CrO_4-ZrO_2 prepared by using a simple technique of coprecipitation and sonication. Prepared HR-SEM materials characterized with an EDX, HR-TEM, XRD, PL and UV–Vis DRS analysis. HR-SEM images demonstrate the prepared materials shown in spherical multi shaped chain structure. (EDX) analysis ensures the nanocomposite material presents of Cr, Zr and O. Analysis of X-ray diffraction studies shows that the synthesized material monoclinic in nature. The PL analysis and UV–Vis DRS analysis were very useful to explain catalytic activity of synthesized particles. This material nanocomposite increases Trypan Blue (TB) dye concentration photocatalytic activity of $1x10^{-4}$ solution at pH 7 Optimal CuO nanomatter. For higher CrO_4-ZrO_2 activity than ZrO_2, a possible mechanism is proposed for 365 nm under UV radiation. $DSSC_S$ analysis showed improved current output, short circuit industrial electrochemical application of CrO_4-ZrO_2 nanocomposite material and prepared CrO_4-ZrO_2 nanocomposite material to be stable and reusable to be concluded with electrochemical properties of synthetic colouration and natural dye.

1. INTRODUCTION
Zirconium oxide nanocrystalline particles exhibit size-dependent properties, novel optical, electronic, magnetic, mechanical properties cannot be achieved using their bulk counterparts **[1-4]**. Zirconium oxide is one of the most intensively studied materials owing to its technologically important applications in oxygen sensors, fuel cells electrolytes, catalyst, and catalytic supports, metal oxides semiconductor devices, superior thermal and chemical stability, etc., **[5]**. Nanostructured Zirconium oxide powders can effectively degrade pollutants. Zirconium oxide can be widely used in the fabrication of structural ceramic devices, gas sensors, catalysts, and optoelectronics devices **[6-8]**.

2. EXPERIMENTAL SECTION
2.1. Materials
The Zirconyl nitrate hydrate, Trypan Blue (TB), $((NH_4)_2Cr_2O_7.2H_2O$, Citric acid, ammonia and ethanol solution and Fluorine doped Tin oxide FTO-plate) and Ruthenium dye (535-bisTBA, N719) solution, it was Sigma Aldrich reagent and was used as such All glassware was cleaned with acid and washed thoroughly with distilled water. Water is used as an experiment throughout. The Trypan Blue (TB) Chemical structure shown in **Fig. 1.**

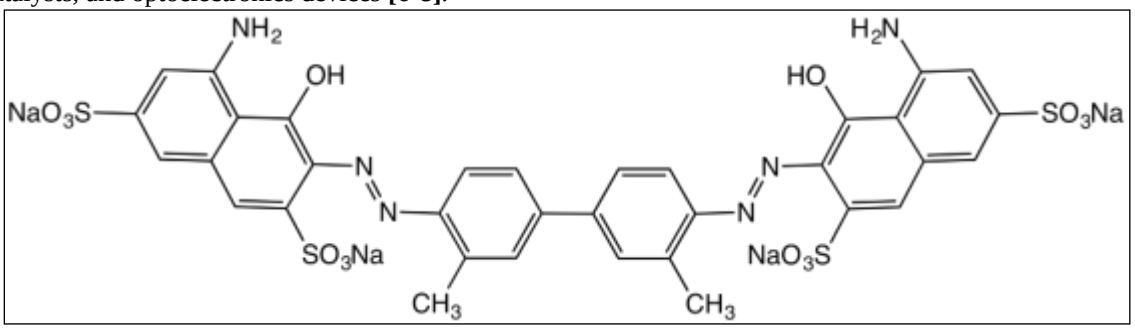

2.2. Synthesis of CrO_4-ZrO_2 nanomaterial
$(NH_4)_2Cr_2O_7.2H_2O$ were first dissolved with distilled water respectively, The resulting solution was added dropwise into Zirconyl nitrate hydrate with ammonia solution added in 1:2 radio. Solution with anhydrous ethanol as solvent at room temperature under vigorous stirring 4 h until precipitate formed was placed in sonication 20 min. The obtained precipitate was filtered and washed with distilled water and ethanol until alkali phases were removed from precipitation. Then the precipitate was collected and dried in oven at overnight. The resulting powder was finally calcined at 150, 300 and 450℃ for 3 h. The prepared

ISSN (Online): 2455-3662
EPRA International Journal of Multidisciplinary Research (IJMR) - Peer Reviewed Journal
Volume: 10| Issue: 3| March 2024|| Journal DOI: 10.36713/epra2013 || SJIF Impact Factor 2024: 8.402 || ISI Value: 1.188

CrO_4-ZrO_2 450℃ heat treatment at a higher photocatalytic activity**.**

2.3. Characterization of CrO_4-ZrO_2 Nanocomposite Material

Ultraviolet and visible (UV–vis) absorbance spectra were measured over a range of 800–200 nm with a Shimadzu UV-1650PC recording spectrometer using a quartz cell with 10 mm of optical path length. High resolution Scanning Electron Microscopy (HR-SEM) as well as Elementary Dispersive X-ray (EDX) evaluation experiments were performed on a FEI Quanta FEG 200 instrument with EDX analyzer facility at 25 ℃. The nanoparticles size and structure verifications were done by Transmission Electron Micro-scopy (HR-TEM) making use of PHILIPS CM200. Each spectrum was recorded with an acquisition time of 18 s. XRD spectrum was recorded on the X'PERT PRO model X-ray diffractometer from Pan Analytical instruments operated at a voltage of 40 kV and also a current of 30 mA with Cu Ka radiation.

Photoluminescence (PL) spectra at a room temperature were recorded using a Perkin-Elmer LS 55 fluorescence spectrometer. UV spectral measurements were done using a Hitachi-U-2001 spectrometer. Ultraviolet and visible (UV–vis) absorbance spectra were measured over a range of 800–200 nm with a Shimadzu UV-1650PC recording spectrometer using a quartz cell with 10 mm of optical path length. The antibacterial activity was studied by disc diffusion method; the test compound was dissolved in DMSO (200 mg/mL) for about half an hour. Commercially available drug disc, Ciprofloxacin (10 mg/ disc) was used as positive reference standard

2.4. Photocatalysis

The photocatalytic activities of CrO_4-ZrO_2 nanocomposite material were evaluated by the photodegradation of dye. The light irradiation at 365 nm. The reaction was carried out at ambient temperature (303 K). The experiment, aqueous suspensions of dye (40 mL, 1×10^{-4} M) and 0.080 g of photocatalyst were loaded in reaction tube of 50 mL capacity with a Prior 60 min in the irradiation, the suspension was magnetically stirred in dark to ensure the establishment of an adsorption or desorption equilibrium. The suspension was kept under constant air-equilibrated condition. At the intervals of given irradiation time. The suspension was measured spectrophotometrically within the theory to Beer–Lambert law limit.

3. RESULTS AND DISCUSSION

3.1. High-Resolution Scanning Electron Microscope Analysis (HR-SEM) & Energy Dispersive Analysis (EDX)

The scanning electron microscope (SEM) is a technique for high-resolution surface imaging. The texture and morphology of the catalyst are critical parameters that influence photocatalytic activity. **Figure 3.1 (a-c**) depicts a close up and an overview of the sample. Obviously. The diameter of these particles is approximately 4 nm, as shown in **Fig.3.1.** Anandhan et al [9] created 8 nm Zirconium oxide nanoparticles with spherical morphology, smooth surfaces, and high catalytic and photochemical activity.

The morphology of prepared CrO_4-ZrO_2 was annealed for three hours at 450 °C. The prepared CrO_4-ZrO_2 nanocomposite material has a spherical-like 3D structure. CrO_4-ZrO_2 nanocomposite material is uniformly distributed on the surface of ZrO_2. Because of its high specific area, the prepared CrO_4-ZrO_2 nanocomposite material with such a structure and morphology is very useful in catalysis.

To determine the elemental composition of the synthesized CrO_4-ZrO_2 nanocomposite material, EDS analysis was performed. The EDS analysis reveals distinct peaks of Cr, O, and Zr atoms, indicating that CrO_4^- has been incorporated with ZrO_2. **Figure.3.1** depicts these findings. **d**.

3.2. HR-TEM Image

A TEM uses energetic electrons to provide morphological, compositional, and crystallographic information on samples. TEM images were used to examine the surface morphology of prepared CrO_4-ZrO_2. As shown in **Fig. 3.2.a**, the sample has nano square structures that resemble spherical shapes with agglomeration, and the diameter of the nano particles is approximately 100 nm. These nanocrystals are visible under magnification. Anandhan et al [10] created 100 nm spherical Tin oxide nanoparticles with electrical, optical, magnetic, high catalytic, and photochemical activity.

At 100 nm magnifications, **Figure 3.2.b** shows the well-resolved lattice fringes. The average particle size distribution is depicted **in Figure 3.2. c.** The **Figure 3.2. d** depicts a selected particle size of 0.21 nm. The particle size observed in TEM studies agrees well with the average size obtained from XRD results. Using the "Image J Viewer" software skills, the image profile and normal particle range distribution were determined.

ISSN (Online): 2455-3662
EPRA International Journal of Multidisciplinary Research (IJMR) - Peer Reviewed Journal
Volume: 10| Issue: 3| March 2024|| Journal DOI: 10.36713/epra2013 || SJIF Impact Factor 2024: 8.402 || ISI Value: 1.188

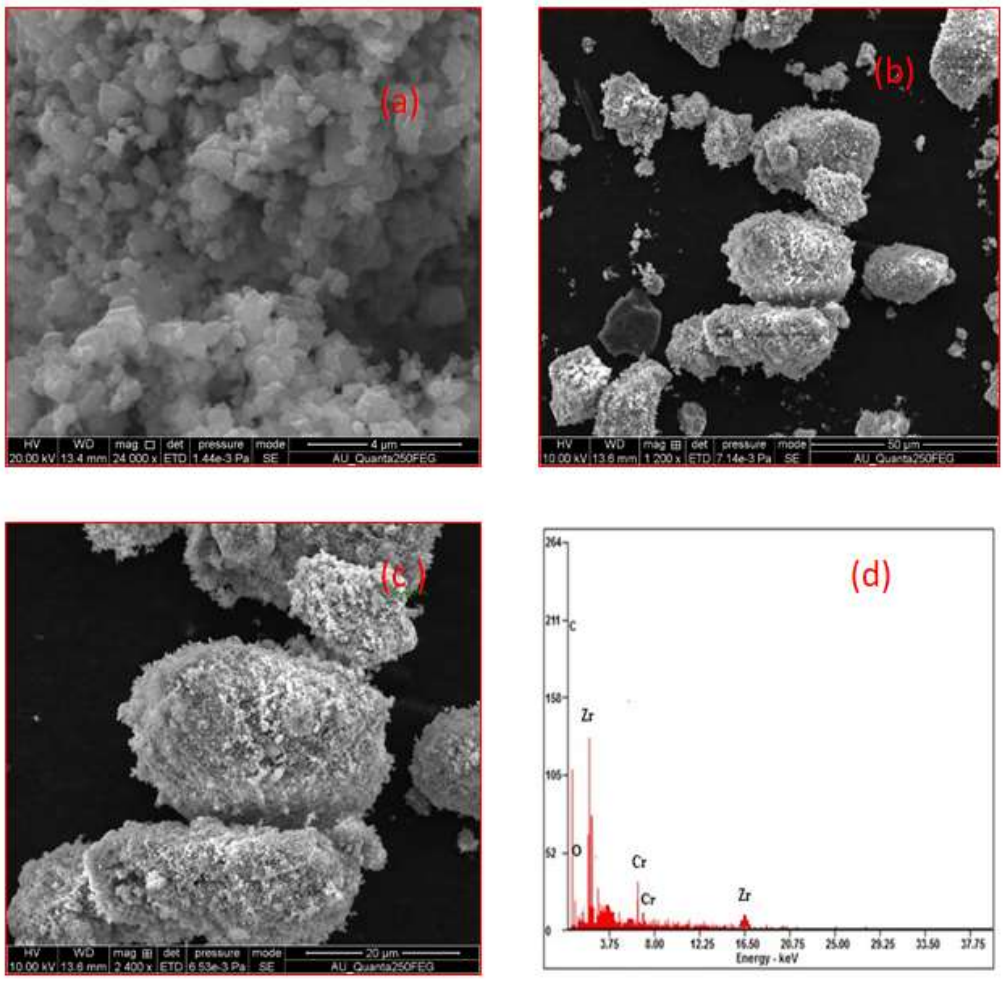

Figure 3.1. HR-SEM image and EDX analysis of CrO_4-ZrO_2 nanocomposite material

ISSN (Online): 2455-3662
EPRA International Journal of Multidisciplinary Research (IJMR) - Peer Reviewed Journal
Volume: 10| Issue: 3| March 2024|| Journal DOI: 10.36713/epra2013 || SJIF Impact Factor 2024: 8.402 || ISI Value: 1.188

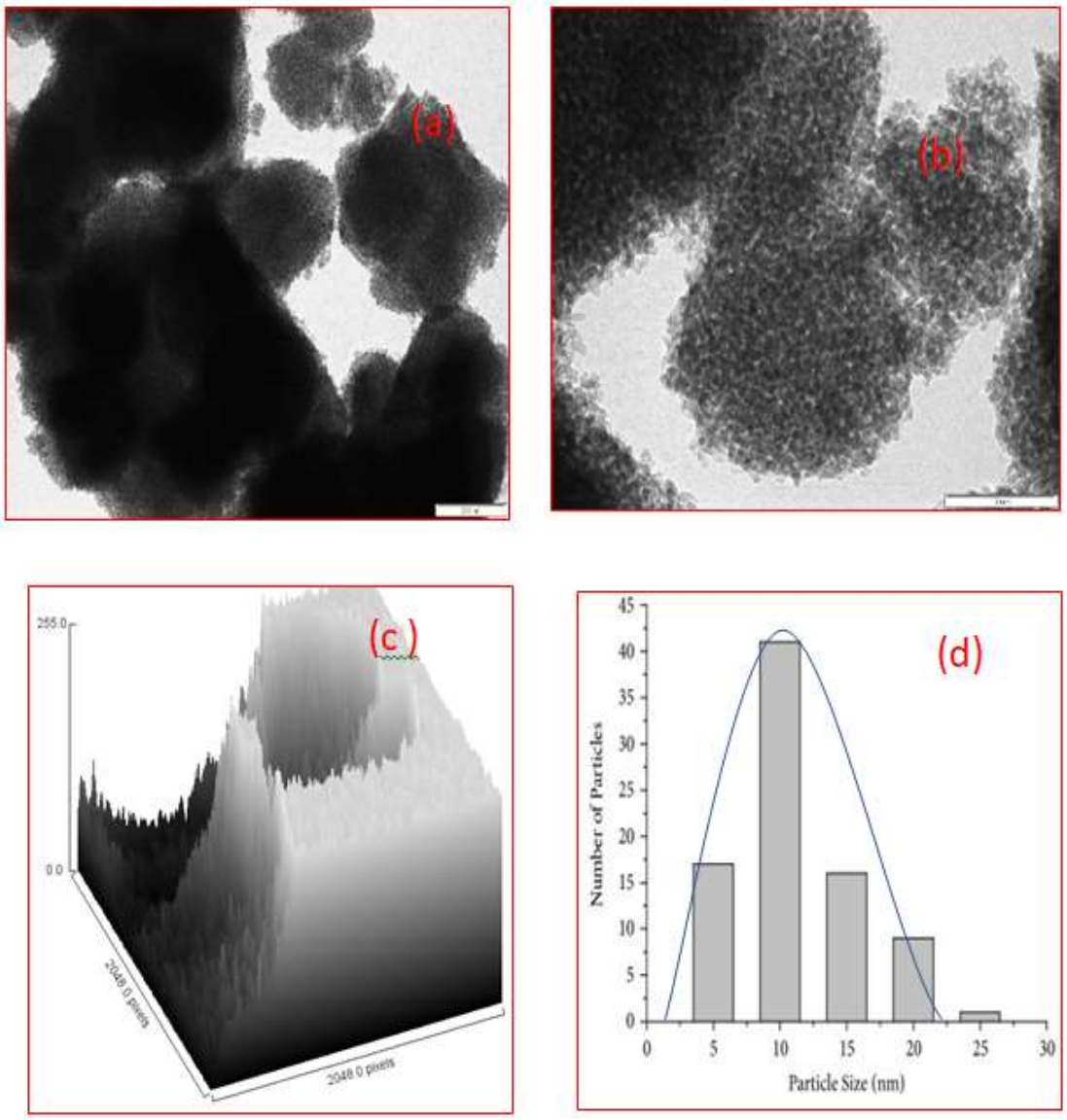

Figure.3.2. HR-TEM analysis of CrO_4-ZrO_2 nanocomposite material (a, b) Image CrO_4-ZrO_2 (c) Surface plot and (d) particle size in selected area highlighted fig (a)

3.3. XRD Analysis

The powder XRD study was carried out to find out crystalline structure of prepared CrO_4-ZrO_2 nanocomposite material. The **Figures 3.3a** and **b** displayed the XRD patterns of bare ZrO_2 and prepared CrO_4-ZrO_2 nanocomposite material. The XRD patterns of ZrO_2 and prepared CrO_4-ZrO_2 showed distinct peaks in the spectrum, the 2θ values at 24.04 °, 28.15 °, 30.00 °, 31.75 °, 35.20 ° and 50.28 °representing (110), (111), (200), (212), (311) and (400) planes, respectively. As indexed in the figure, all the diffraction patterns indicate the monoclinic structure [JCPDS number 37-1484]. Tokeer Ahmed et al [11] synthesized zirconium oxide nanoparticles have monoclinic structure with 27nm particle size. The peaks of the graph are in good agreement with the literature report. The XRD patterns of the CrO_4 show the new peaks at 33.30 and (101) plane for prepared CrO_4-ZrO_2 nanocomposite material. The average Crystallite size of nanocomposite material is calculated from in Debye–Scherrer formula,

$$D = K\lambda / \beta \cos \Theta \quad \text{..... (1.1)}$$

Where, D = crystalline size of the nanocomposite material
K = shape factor (or) Dimensionless constant
λ = Wavelength of the X-rays
β = the full line width at the half-maximum elevation of the main intensity peak (FWHM), and
Θ = Bragg diffraction angle. Since this equation,

ISSN (Online): 2455-3662
EPRA International Journal of Multidisciplinary Research (IJMR) - Peer Reviewed Journal
Volume: 10| Issue: 3| March 2024|| Journal DOI: 10.36713/epra2013 || SJIF Impact Factor 2024: 8.402 || ISI Value: 1.188

The crystalline size of ZrO_2 nanocomposite material and prepared CrO_4-ZrO_2 nanocomposite material was calculated about 27 nm and 19 nm correspondingly.

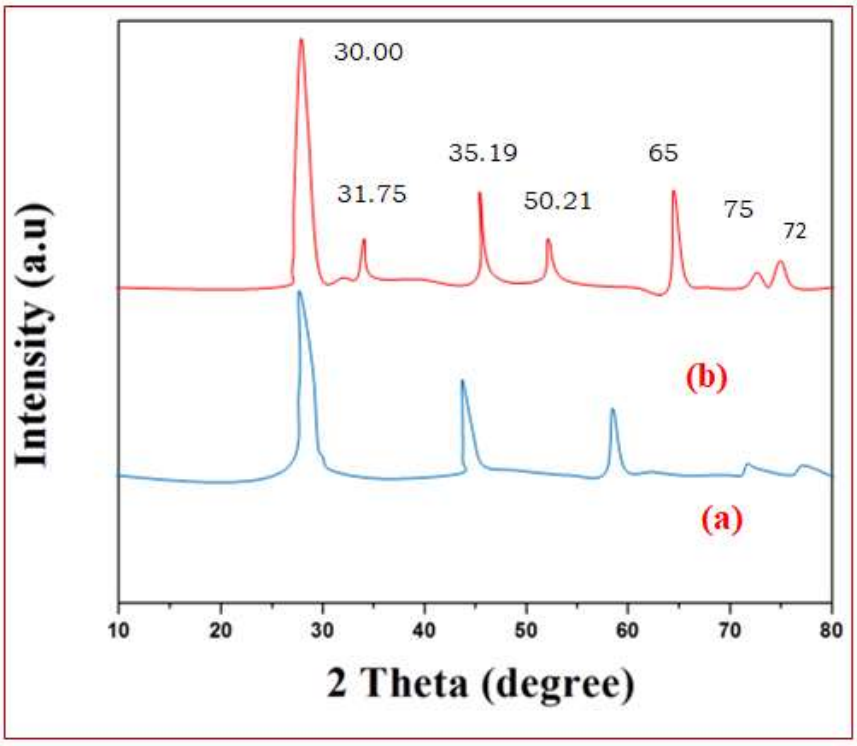

Figure. 3.3. XRD pattern of (a) ZrO_2 and (b) CrO_4- ZrO_2 nanocomposite material

3.4. PL Spectral Analysis

The electronic structure, transfer behaviour, and recombination rate of photoexcited electron-hole pairs in semiconductor materials can all be studied using photoluminescence spectroscopy (PL). Irradiative recombination of photoexcited electrons and holes produces the PL spectra. These charge carriers are crucial in determining the efficiency of photocatalytic activity.

As a result of the Photoluminescence spectra used to read the transfer, movement, and recombination processes of the photogenerated electron-hole pairs [12,13], the Photoluminescence spectra emission in nanocomposite material arises from the recombination of without charge carrier**. Figures 3.4. a and b** depict the PL spectrum of ZrO_2 and the prepared CrO_4-ZrO_2 nanocomposite material, with excitation wavelengths of 320 and 435 nm, respectively. It is primarily composed of two emission bands: a strong blue emission band at 320 nm and a green emission band at 435 nm. Feng Gu et al [14] reported a blue band at approximately 423 nm, as well as a green band at 535 nm; these values agree with the above result.

The intensity of CrO_4^- doped ZrO_2 is lower than that of pure ZrO_2, implying that the electron-hole recombination rate is much lower and the separation efficiency is much higher in the doped sample. The PL emission bands observed in current ZrO_2 may be caused by transitions from surface trap states in the conduction band to lower energy levels near the valance band. This is consistent with the findings reported in the literature [15,16]. The small particle size was the main reason for the broad fluorescence band, according to the very narrow particle size distribution [17,18]. The bands observed at 220 nm and 435 nm might be due to the presence of oxygen vacancies [19].

ISSN (Online): 2455-3662
EPRA International Journal of Multidisciplinary Research (IJMR) - Peer Reviewed Journal
Volume: 10| Issue: 3| March 2024|| Journal DOI: 10.36713/epra2013 || SJIF Impact Factor 2024: 8.402 || ISI Value: 1.188

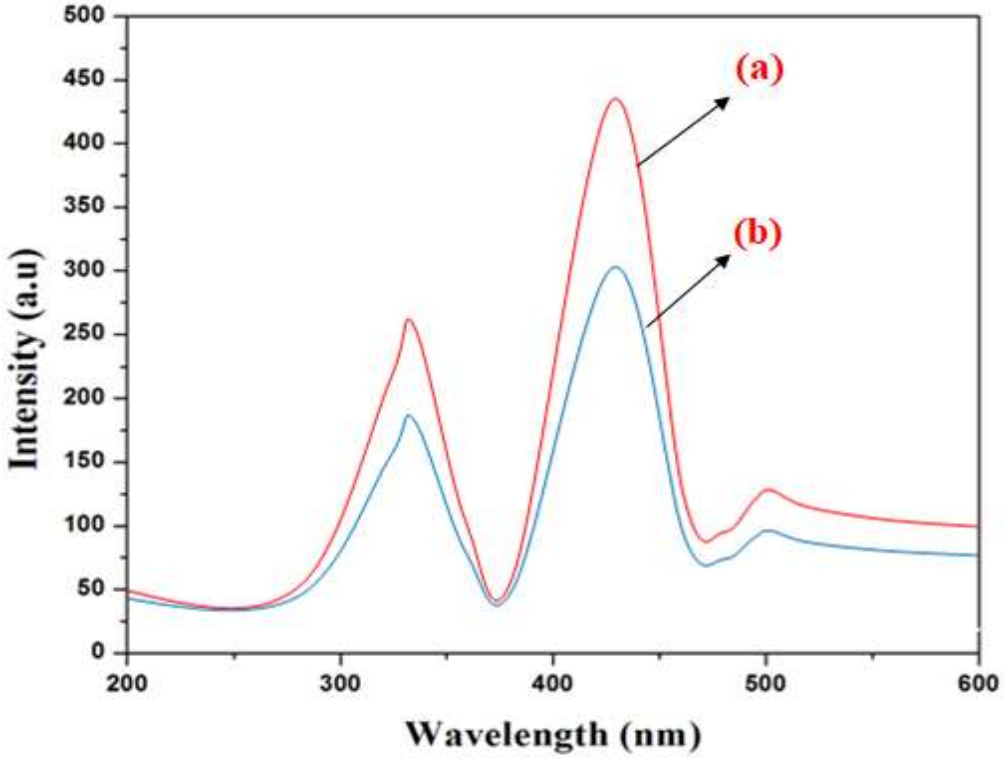

Figure. 3.4. PL analysis of (a) ZrO_2 and (b) CrO_4- ZrO_2 nanocomposite material

3.5. Diffuse Reflectance Spectroscopy

The UV-Vis DRS analysis is one of the spectra analysis show regions in a specific wavelength range which can be attributed to the photo-excitation of electrons from VB to CB. The UV-Vis can be approximately calculated from the optical reflectance data by the Kubelka–Munk function,

$$A = F(R) = \frac{((1-R)^2)}{2R} \quad \ldots\ldots (1.2)$$

where α is the absorbance coefficient,
R is the diffuse reflectance (6). An extrapolation of the linear region of a plot of (F(R) hv)2 vs hv gives the value of the optical bandgap energy. The bandgap energy for nanocomposite material is calculated from E = hν = hc/λ.

ISSN (Online): 2455-3662
EPRA International Journal of Multidisciplinary Research (IJMR) - Peer Reviewed Journal
Volume: 10| Issue: 3| March 2024|| Journal DOI: 10.36713/epra2013 || SJIF Impact Factor 2024: 8.402 || ISI Value: 1.188

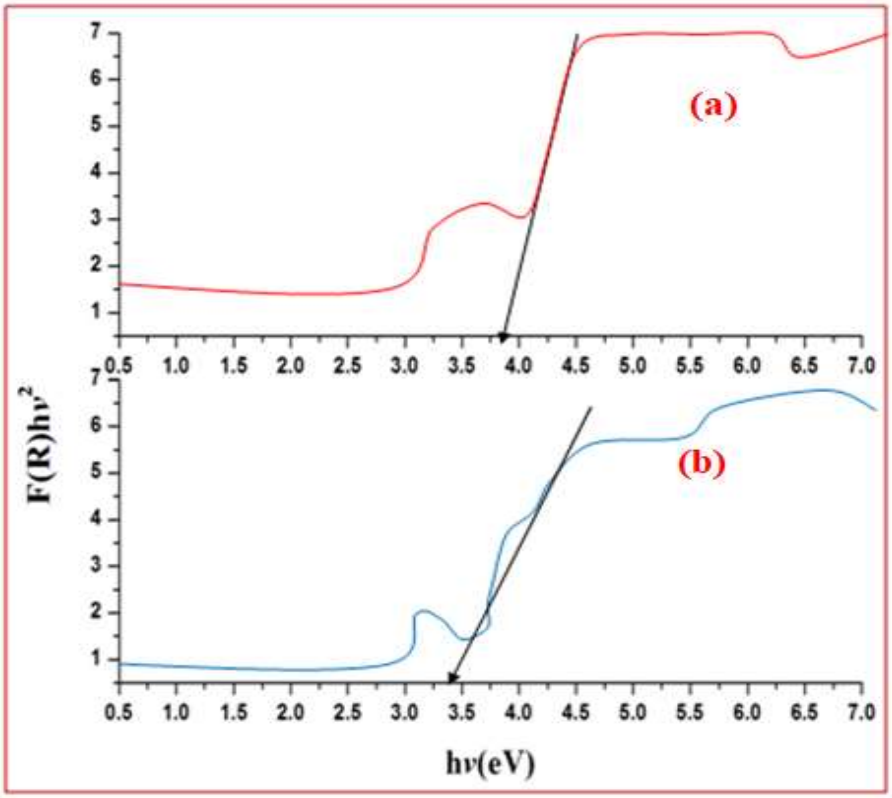

Figure. 3.5. UV-Vis DRS analysis of (a) ZrO_2 and (b) CrO_4-ZrO2 nanocomposite material

The bandgap energy of pure ZrO_2 and prepared CrO_4-ZrO_2 nanocomposite material is 3.19 and 3.0 eV correspondingly its shows in Figure 3.5 a and b. These results showing prepared CrO_4-ZrO_2 nanocomposite material has low bandgap low bandgap energy high photocatalyst and electrochemical applications were obtained [20].

3.6. Photocatalytic application under solar and UV-light

3.6.1. Primary Analysis; Photodegradation Study of TB Dye

Figures 3.6.1 A and B show the photo degradability of Trypan Blue (TB) with various photocatalysts under UV and solar light. In the absence of UV and solar light, the percentage of dye degradation with CrO_4-ZrO_2 is very low (curve-a). This could be due to dye adsorption on the catalyst's surface. The curve-b depicts the degradation of dye in the absence of a photocatalyst under UV and solar light. Self-photolysis is not a problem for dye. These findings suggest that both UV and solar light are required for the effective degradation of Trypan Blue (TB) dye. Under UV and solar light, the percentages of dye degradation with ZrO_2 are 36% and 39%, respectively (curve-c). Under UV and solar light, the percentage of dye degradation with prepared CrO_4-ZrO_2 is 65% and 68%, respectively (curve-d). This demonstrates that prepared CrO_4-ZrO_2 degrades Trypan Blue (TB) more efficiently under solar light.

ISSN (Online): 2455-3662
EPRA International Journal of Multidisciplinary Research (IJMR) - Peer Reviewed Journal
Volume: 10| Issue: 3| March 2024|| Journal DOI: 10.36713/epra2013 || SJIF Impact Factor 2024: 8.402 || ISI Value: 1.188

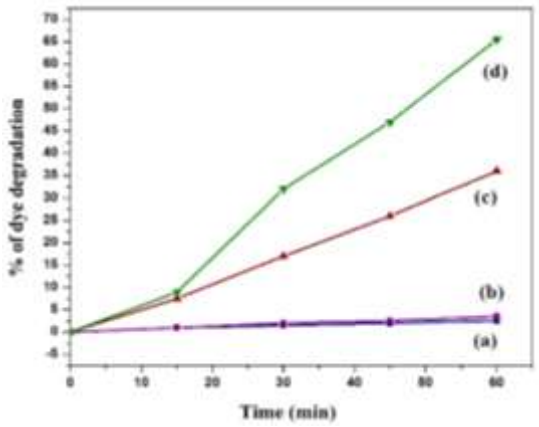

Figure 3.6.1. (A) . Photodegradation study of TB dye under UV-light - irradiation at 365 nm by (a) Dark (b) Nil catalysis (c) ZrO_2 (d) CrO_4- ZrO_2 nanocomposite material

- TB dye $1x10^{-4}$, nanocomposite material suspended=2 gL $^{-1}$, airflow rate 8.1 mL s $^{-1}$, IUV =1.381×10^{-6}Einstein L $^{-1}$ S $^{-1}$

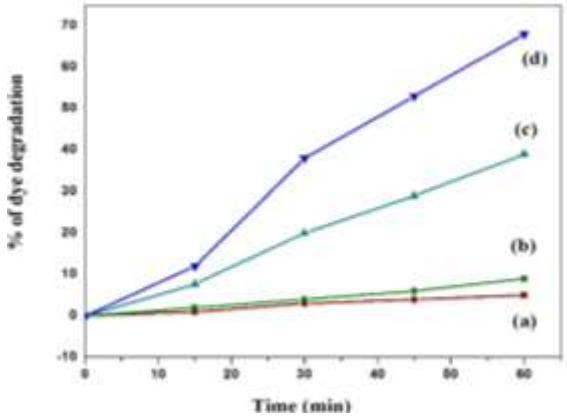

Figure 3.6.1. (B) . Photodegradation study of TB dye under Solar light irradiation at 365 nm by (a) Dark (b) Nil catalysis (c) ZrO_2 (d) CrO_4- ZrO_2 nanocomposite material

- TB dye $1x10^{-4}$, nanocomposite material suspended=2 gL $^{-1}$, airflow rate 8.1mL s $^{-1}$, Isolar= 1250 × 100±100 Lux.

3.6.2. Effect of pH on photodegradation of dye

The pH of the solution has a significant impact on photocatalytic activity. The surface properties of the ZrO_2 and prepared CrO_4-ZrO_2 catalyst are significantly affected by the pH of the reaction medium. The pH of the solution has a significant impact on photocatalytic activity. The surface properties of the ZrO_2 and prepared CrO_4-ZrO_2 catalyst are significantly affected by the pH of the reaction medium. **Figures 3.6.2 A and B** depict the effect of pH on trypan blue photocatalytic degradation. The figure clearly shows that the photocatalytic process is highly dependent on the pH of the dye solution [21].

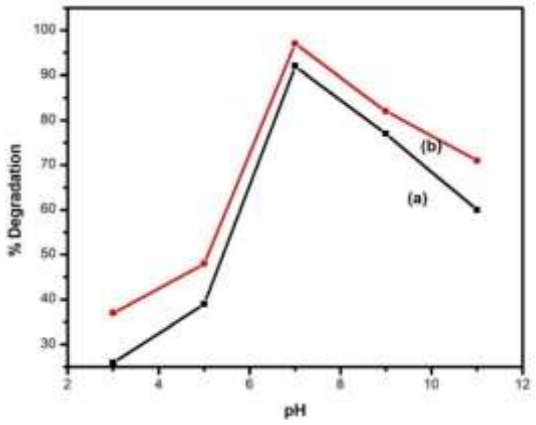

Figure 3.6.2. (A) pH study under UV-light **(**a) ZrO_2 and (b) CrO_4- ZrO_2 nanocomposite material.

- TB dye $1x10^{-4}$, nanocomposite material suspended=2 gL $^{-1}$, airflow rate 8.1 mL s $^{-1}$, IUV =1.381×10^{-6}Einstein L $^{-1}$ S $^{-1}$

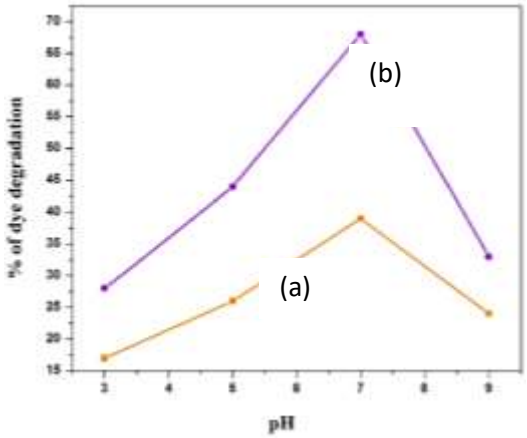

Figure 3.6.2. (B) pH study under Solar light **(**a) ZrO_2 and (b) CrO_4- ZrO_2 nanocomposite material.

- TB dye $1x10^{-4}$, nanocomposite material suspended=2 gL $^{-1}$, airflow rate 8.1mL s $^{-1}$, Isolar= 1250 × 100±100 Lux.

The pH changes the surface properties of the nanocomposite material, causing the dye molecules to dissociate. At pH 7, per hydroxyl radicals ($HO_2^{\bullet}$) are formed, which results in the formation of hydrogen peroxide, which produces several hydroxyl radicals ($HO^{\bullet}$) [22]. At pH 7, the highest photocatalytic degradation of ZrO_2 and prepared CrO_4 ZrO_2 is observed. It has

ISSN (Online): 2455-3662
EPRA International Journal of Multidisciplinary Research (IJMR) - Peer Reviewed Journal
Volume: 10| Issue: 3| March 2024|| Journal DOI: 10.36713/epra2013 || SJIF Impact Factor 2024: 8.402 || ISI Value: 1.188

been discovered that degradation is strongly influenced by the pH of the solution. The percentage of degradation is observed to increase up to pH 7 and then decrease. Under UV and solar light, pH 7 has superior photocatalytic activities.

3.6.3. Effect of Temperature on photodegradation of dye

Temperature effects on catalytic reaction of CrO_4-ZrO_2 nanocomposite material were studied from 150 °C to 450 °C. As the reaction temperature was raised, the equilibrium of TB removal was reached in less time, as shown in **Figures 3.6.3 A and B**. The highest percentage degradation was observed at 450°C, where 65% and 68% of TB were removed after only 60 minutes under UV and solar light, respectively. The lowest percentage degradation was observed at 300 °C, where 28% and 31% of TB were removed after only 60 minutes under UV and solar light, respectively. The lowest percentage degradation was observed at 150 °C, where 21% and 23% of TB were removed after only 60 minutes under UV and solar light, respectively. At high temperatures, hydrogen peroxide easily self-decomposes, and the decomposition rate of hydrogen peroxide increases with every 150 °C. Superior temperatures tend to reduce the number of defects on the photocatalyst's surface area.

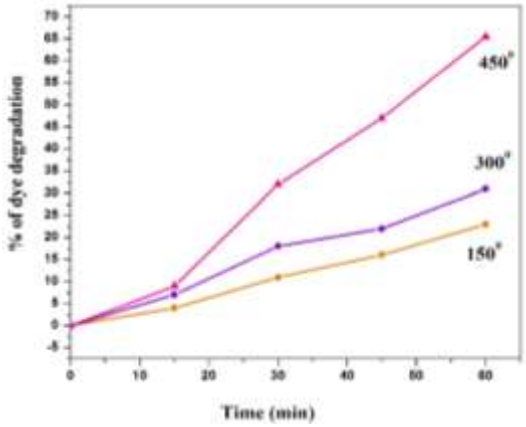

Figure 3.6.3. (A) The effects of Temperature under UV-light CrO_4- ZrO_2 nanocomposite material (a, b)

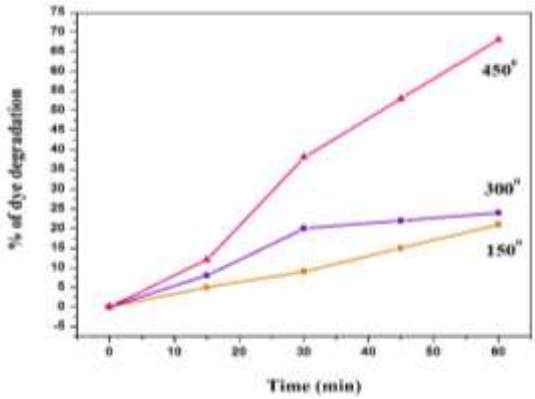

Figure 3.6.3. (B) The effects of Temperature under Solar light CrO_4- ZrO_2 nanocomposite material (a, b)

- TB dye $1x10^{-4}$, nanocomposite material suspended=2 gL^{-1}, airflow rate 8.1 mL s^{-1}, IUV =1.381×10^{-6}Einstein L^{-1} S^{-1}
- TB dye $1x10^{-4}$, nanocomposite material suspended=2 gL^{-1}, airflow rate 8.1mL s^{-1}, Isolar= 1250 × 100±100 Lux.

Effect of Catalyst Loading on photodegradation of dye

The effect of catalyst loading investigated from 0.05, 0.08 and 0.10g of ZrO_2 and prepared CrO_4- ZrO_2 nanocomposite material photodegradation of TB dye ($1x10^{-4}$ M) solution used UV and solar- Light degradation at 365 nm on 60 min and time interval 15 min obtained. The utmost degradation of TB dye under UV and solar light exhibit 0.05g on ZrO_2 at (16 % & 24 %), 0.08 g (36 % & 39 %), 0.1 g (24 % & 49 %) and prepared CrO_4- ZrO_2 degradation of TB dye exhibit0.05 g (16 % & 19 %), 0.08 g (65 % & 68 %), 0.1g (10 % & 46 %). **Figures 3.6.4 A and B** show the effect of catalyst load on the photocatalytic degradation of the dye.

The catalytic (ZrO_2 and CrO_4-ZrO_2) load was varied from 0.05 to 0.1 g/ 50 mL to determine the optimal catalyst dosage. The ideal load was determined to be 0.08 g/50 mL. A screening effect may occur if the catalyst loading is increased beyond the optimal dosage. This effect reduces the catalyst's specific activity. Particle aggregation may reduce catalytic activity at higher catalyst dosages. Above the optimal load, slurry turbidity increases, light penetration decreases, and the availability of hydroxides and superoxides decreases; thus, photocatalytic activity decreases. As a result, the optimum catalyst dosage under UV and solar light was 0.08 g/50 mL for the efficient removal of Trypan Blue (TB) dye [23,24].

ISSN (Online): 2455-3662
EPRA International Journal of Multidisciplinary Research (IJMR) - Peer Reviewed Journal
Volume: 10| Issue: 3| March 2024|| Journal DOI: 10.36713/epra2013 || SJIF Impact Factor 2024: 8.402 || ISI Value: 1.188

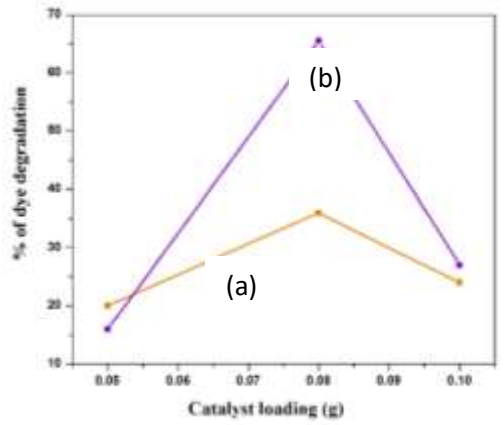

Figure 3.6.4. (A). The effects of catalyst loading (a) ZrO_2 and (b) CrO_4- ZrO_2 nanocomposite material under UV-light.

- TB dye $1x10^{-4}$, nanocomposite material suspended=2 gL^{-1}, airflow rate 8.1 mL s^{-1}, IUV =1.381×10^{-6}Einstein L^{-1} S^{-1}

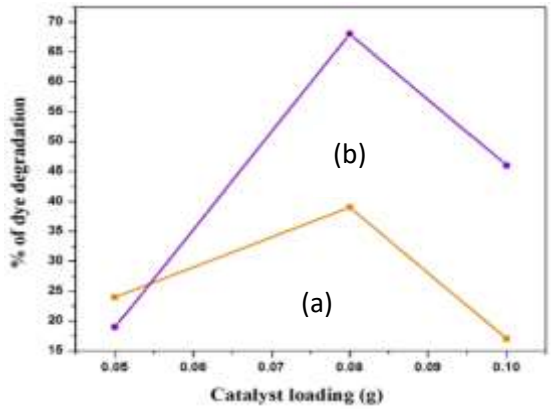

Figure 3.6.4 (B). The effects of catalyst loading (a) ZrO_2 and (b) CrO_4- ZrO_2 nanocomposite material under Solar light

- TB dye $1x10^{-4}$, nanocomposite material suspended=2 gL^{-1}, airflow rate 8.1mL s^{-1}, Isolar= 1250 × 100±100 Lux.

3.6.4. Effect of Dye Concentration on photodegradation of dye

The impact of different initial dye concentrations on photocatalytic degradation has been studied. **Figures.3.6.5 A and B** depict the effect of dye concentration on the photocatalytic activity of ZrO_2 and a CrO_4-ZrO_2 nanocomposite material. Trypan blue was tested at concentrations ranging from $1x10^{-4}$ M to $3x10^{-4}$ M. The catalytic load was kept constant at 0.08 g and the pH was kept at 7. Under UV and solar light, the optimal dye concentration of ZrO_2 and prepared CrO_4-ZrO_2 nanocomposite material was observed to be 1 x 10^{-4} M. The time required for complete dye degradation increases as the dye concentration increases. When the dye concentration is low, many active sites in the photocatalyst are vacant, and the slurry remains almost clear, allowing light to pass through.

Photodegradation is aided by light penetration. The dye molecules occupy the active sites as the dye concentration increases, and this trend continues until all of the sites are filled, which occurs at a specified optimum concentration. Beyond this concentration, the slurry becomes turbid, preventing light penetration and thus slowing degradation. A significant amount of UV and solar-light may be absorbed by the dye molecules rather than the catalyst at high concentrations, reducing catalytic efficiency [25]. Under UV and solar light, the optimum dye concentration of ZrO_2 and prepared CrO_4-ZrO_2 nanocomposite material was observed to be 1 x 10^{-4}M.

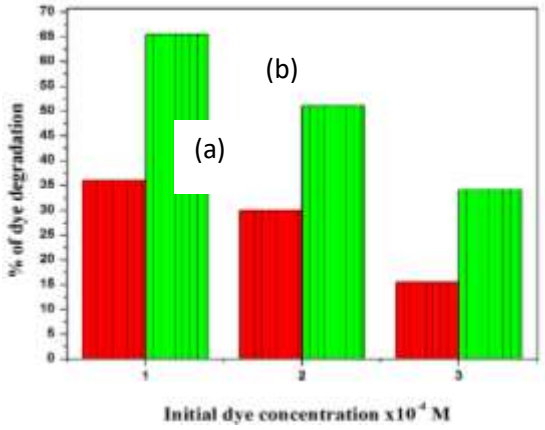

Figure 3.6.5. (A) The effects of concentrations of (a) ZrO_2 and (b) CrO_4- ZrO_2 nanocomposite material under UV-light.

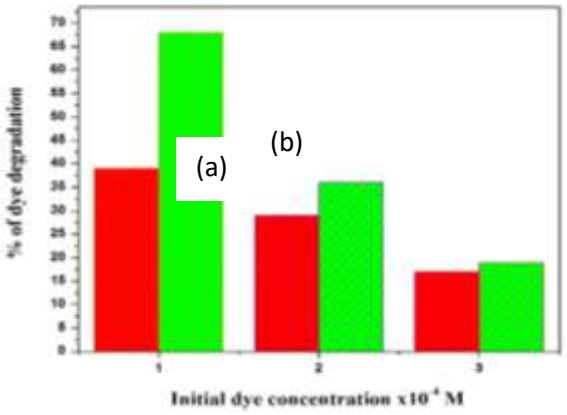

Figure 3.6.5 (B) The effects of concentrations of (a) ZrO_2 and (b) CrO_4- ZrO_2 nanocomposite material under Solar light

ISSN (Online): 2455-3662
EPRA International Journal of Multidisciplinary Research (IJMR) - Peer Reviewed Journal
Volume: 10| Issue: 3| March 2024|| Journal DOI: 10.36713/epra2013 || SJIF Impact Factor 2024: 8.402 || ISI Value: 1.188

- TB dye $1x10^{-4}$, nanocomposite material suspended=2 gL^{-1}, airflow rate 8.1 mL s^{-1}, IUV =1.381×10^{-6}Einstein L^{-1} S^{-1}

- TB dye $1x10^{-4}$, nanocomposite material suspended=2 gL^{-1}, airflow rate 8.1mLs $^{-1}$, Isolar= 1250 × 100±100 Lux.

3.6.5. Stability and Reusability of Photocatalyst

On TB dye, the stability and reusability of ZrO_2 and prepared CrO_4-ZrO_2 nanocomposite material. TB dye degradation experiments were also repeated four times on the nanocomposite material. The nanocomposite material was thoroughly washed in water after each cycle, and a fresh solution of TB dye was made before each photocatalyst run in the photoreactor. **Figures. 3.6.6 A and B** show the results of UV and solar-light irradiation. The complete degradation of TB dye in ZrO_2 and prepared CrO_4- ZrO_2 nanocomposite material under UV and solar light are 74 % & 88 %, 58 % & 80 %, 58 % & 80 %, 58 % & 80 % and 94 % & 95 %, 73 % &81.5 %, 73 % & 81.5 %, 73 % & 81.5 % respectively. **(Table 1.1**). The results indicate prepared catalysts are stable and reusable of nanocomposite material. This suggests that prepared CrO_4-ZrO_2 photocatalyst have stability and reusability for the photodegradation of pollutants **(Table-1.1).** The final result indicates Solar-Light irradiation highly photocatalytic activity than that of UV - Light irradiation

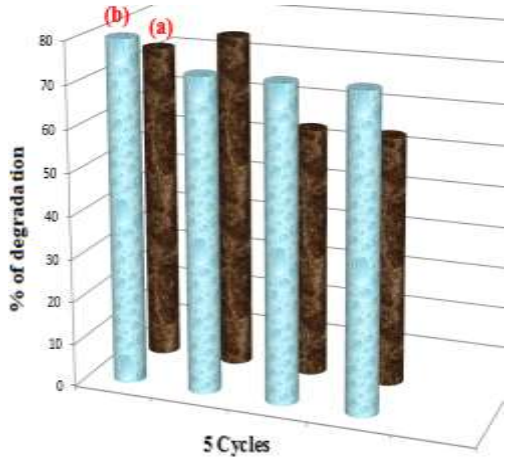

Figure 3.6.6. (A) Stability and Reusability on TB dye degradation; (a) ZrO_2 and (b) CrO_4- ZrO_2 nanocomposite material under UV-light.

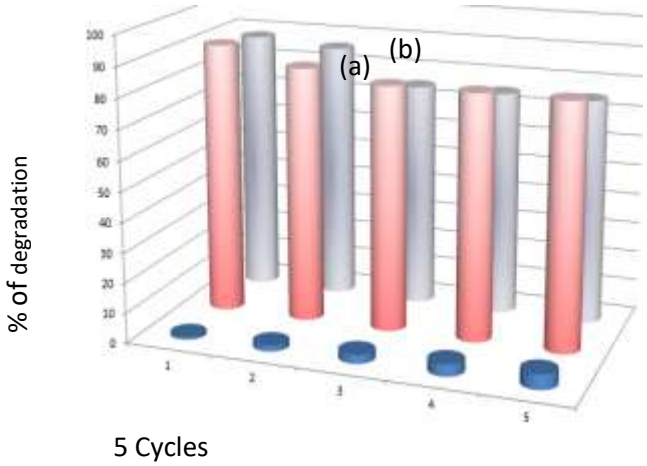

Figure 3.6.6. (B) Stability and Reusability on TB dye degradation; (a) ZrO_2 and (b) CrO_4- ZrO_2 nanocomposite material under Solar light.

- TB dye $1x10^{-4}$, nanocomposite material suspended=2 gL^{-1}, airflow rate 8.1 mL s^{-1}, IUV =1.381×10^{-6}Einstein L^{-1} S^{-1}

- TB dye $1x10^{-4}$, nanocomposite material suspended=2 gL^{-1}, airflow rate 8.1mL s^{-1}, Isolar= 1250 × 100±100 Lux.

Table 1.1 Nano Catalyst Reusability under UV & Solar light

No of cycles	Percentage of TB removal on ZrO_2		Percentage of TB removal on CrO_4- ZrO_2	
	UV	Solar	UV	Solar
1	74	88	94	90.5
2	58	80	73	81.5
3	58	80	73	81.5
4	58	80	73	81.5

4. MINERALIZATION STUDY

4.1. Chemical Oxygen Demand Analysis (COD)

The chemical oxygen demand (COD) analysis is an important indicator of organic pollution in water. The COD measurement for the degradation of Trypan Blue (TB) dye on prepared CrO_4-ZrO_2 nanocomposite material loading amount of 0.08 gram on dye initial concentration $1x10^{-4}$ M suspension for 40 mL of PH 7 solution and air passing with UV 365 nm was performed. The chemical oxygen demand test is a popular method for determining the organic strength of wastewater. The waste can be measured in terms of the total amount of oxygen required for the oxidation of organic matter to CO_2 and water. The dye solution's COD before and after treatment was calculated. The reduction in COD values of the treated dye solution indicates dye molecule mineralization as well as color removal. COD values of blank and treated dye solutions are shown in **Table 1.2**.

ISSN (Online): 2455-3662
EPRA International Journal of Multidisciplinary Research (IJMR) - Peer Reviewed Journal
Volume: 10| Issue: 3| March 2024|| Journal DOI: 10.36713/epra2013 || SJIF Impact Factor 2024: 8.402 || ISI Value: 1.188

Table 1.2. Percentage of chemical oxygen demand analysis of Trypan Blue (TB)

Sl. No.	Time (Min)	COD Values		% of degradation of Trypan Blue with CrO_4-TiO_2
		Initial COD (mg/50mL)	Final COD (mg/50mL)	
1	60	4.5	1.4	68

4.2. Mechanism of Degradation

From the photocatalytic mechanism results, a process based on photocarrier transfer is discovered. With 365 nm light, ZrO_2 is excited upon irradiation. The transfer of the photoexcited electron from the surface of CrO_4- ZrO_2 nanoflower occurs in the case of CrO_4 altered ZrO_2 due to greater positive conduction band potential. The charge carriers are thus effectively separated Electrons stored on the nanocomposite material conduction band are absorbed by adsorbed O_2 molecules. The result is supper oxide radicals ($O2^{-\bullet}$) being formed TB dye molecules are decomposed by these superoxide radicals and hydroxide radicals formed by holes [26-29]. It is shown in **Scheme 1.1**.

5. ELECTRO CATALYTIC APPLICATION

5.1. Dye sensitized solar cells Analysis

The **Figures.5.1 a and b** show that the fabrication activity of photo current-voltage (I-V) in the sensitized solar cells (DSSCs) dye as photoelectrode, as photoelectrodes are coated on the fluorine-doped tin oxide (FTO-plate) glass substrate, ZrO_2 and prepared CrO_4- ZrO_2 nanocomposite material act as photoelectrode. The routine solar cell is fabricated with ZrO_2 and prepared CrO_4-ZrO_2 nanocomposite material with Ruthenium dye (535-bisTBA, N719). From the data, it is clear that (N719) the prepared CrO_4- ZrO_2 nanocomposite material-based cell gives the brilliant activity with the use of dye as sensitizer reunite the maximum value of short-circuit current density, Jsc (3.2 mA/cm ^{2}) than ZrO_2 (3.0 mA/cm ^{2}), open-circuit voltage, Voc (500 mV), fill-factor, FF (0.94 and efficiency, η (1.7 %).

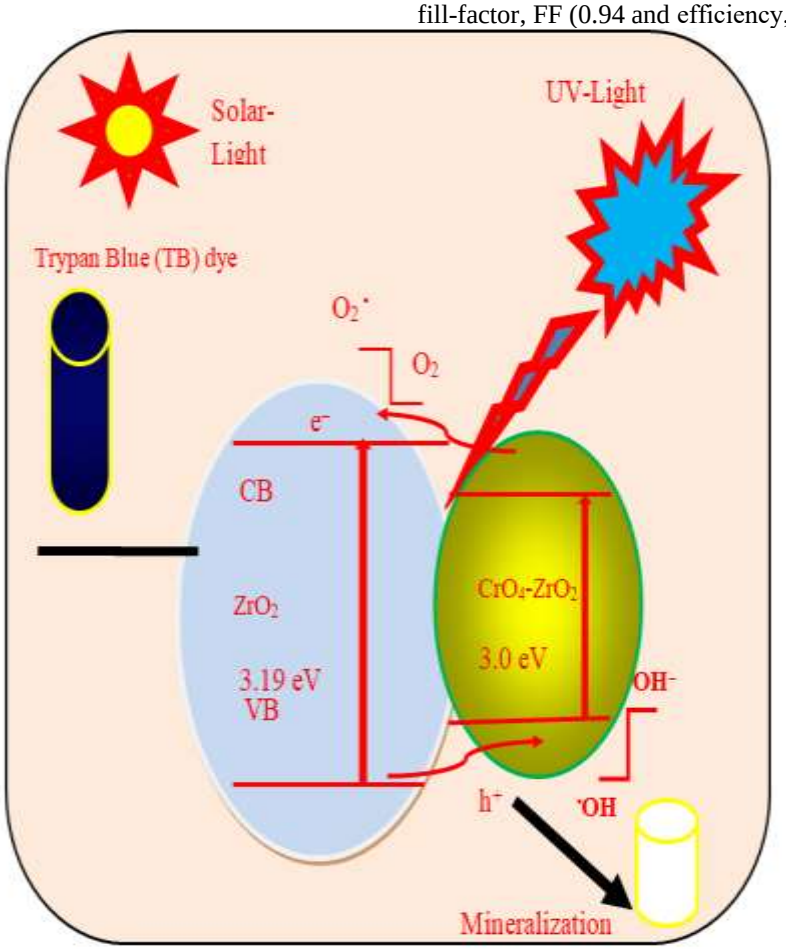

ISSN (Online): 2455-3662
EPRA International Journal of Multidisciplinary Research (IJMR) - Peer Reviewed Journal
Volume: 10| Issue: 3| March 2024|| Journal DOI: 10.36713/epra2013 || SJIF Impact Factor 2024: 8.402 || ISI Value: 1.188

Scheme. 1.1. Schematic representation for the photodegradation holes and electrons in the nanocomposite material under Solar and UV- light for successive mineralization of TB dye.

The outcome indicates successful electron transfer of prepared CrO_4-ZrO_2 nanocomposite material and keeps back the recombination of the photogenerated charge carrier, thus increasing the short circuit current and electron transfer [30].

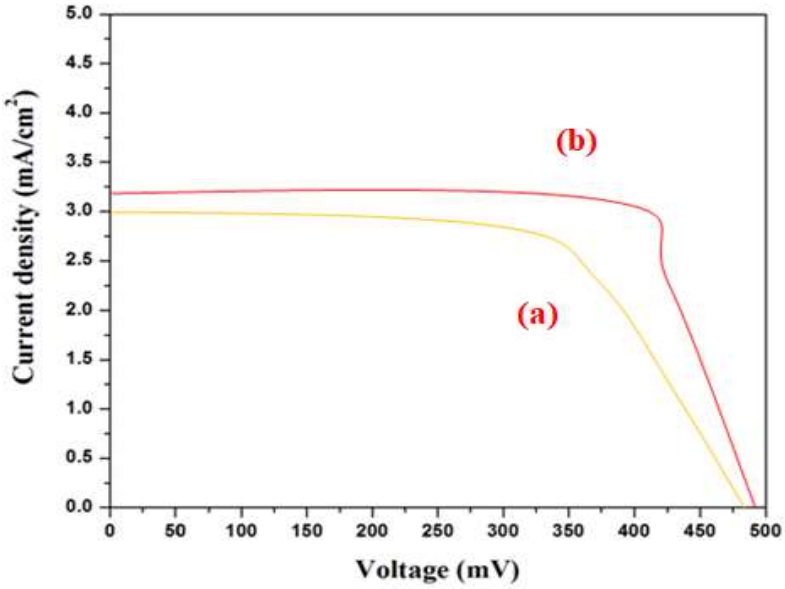

Figure 5.1. Current density–voltage (I–V) curves for the DSSC's fabricated from (a) ZrO_2 and (b) CrO_4- ZrO_2 nanocomposite material

6. CONCLUSION

The prepared CrO_4-ZrO_2 nanocomposite material was synthesized using a co-precipitation method and was characterized by HR-SEM and HR-TM analysis for spherical morphology structure, with X-ray (EDX) analysis confirming the presence of Cr, Zr, and O in the nanocomposite material. The crystalline size of both ZrO_2 and prepared CrO_4- ZrO_2 was determined using the Debye-Scherrer equation. XRD analysis revealed that the average crystalline size of ZrO_2 and prepared CrO_4- ZrO_2 is 27 nm and 19 nm, respectively. The decrease in PL (CrO_4-ZrO_2) intensity results in high photocatalytic activity comparable to ZnO_2. The UV-Vis DRS spectrum had a low bandgap energy, allowing it to function as an efficient photocatalyst and to be used in DSSCS applications. The photocatalytic application of TB dye under Solar-Light irradiation is more photocatalytic than that under UV-Light irradiation. The prepared nanomaterial was found to be stable and reusable after an achievable mechanism was proposed and the nanomaterial was discussed extensively. According to the electrochemical analysis results, the prepared CrO_4-ZrO_2 nanocomposite material is effective in electron transfer and inhibits photogenerated charge carrier recombination, which improves electron transfer and increases short circuit current.

Credit authorship contribution statement

K. Subashri: Writing - original draft, Writing - review & editing, Conceptualization, Data curation, Methodology.

Declaration of Competing Interest

The authors declare that they have no known competing financial interests or personal relationships that could have appeared to influence the work reported in this paper.

REFERENCE

1. *A.P. Alivisatos, Semiconductor Clusters, Nanocrystals, and Quantum Dots, Science 271, 933-937, 1996.*
2. *S.A. Majetich and Y. Jin, Magnetization Directions of Individual Nanoparticles, Science 284, 470-473, 1999.*
3. *K. Gupta, P.C. Jana and A.K. Meikap, Synthesis and properties of polyaniline samarium nanocomposite, J. Phys. Sci., 16, 209-216, 2012.*
4. *K. Anandan and V. Rajendran, Rose-like SnO_2 nanostructures synthesized via facile solvothermal technique and their optical properties, J. Phys. Sci., 14, 227-234, 2010.*
5. *R.J. Liu, Y. Li, H. Zhao, F.Y. Zhao and Y.Q. Hu, Synthesis and characterization of Al_2O_3 hollow spheres, Mater. Lett., 62, 2593-2595, 2008.*
6. *Tahir, M.N.; Gorgishvili. L.; J.; Gorelik, T.; Kolb, U.; Nasdala, L.; Tremel, W. Facile synthesis and characterization of monocrystalline cubic ZrO_2 nanoparticles. Solidstate Sci. 9, 1105 – 1109, 2007.*

ISSN (Online): 2455-3662
EPRA International Journal of Multidisciplinary Research (IJMR) - Peer Reviewed Journal
Volume: 10| Issue: 3| March 2024|| Journal DOI: 10.36713/epra2013 || SJIF Impact Factor 2024: 8.402 || ISI Value: 1.188

7. *Rozoa, C.; Jaque, D.; Fonceca, L.F.; Gracia Sole, J. Luminescence of rare earth doped Si-ZrO2 co-sputteread films. J. Lumin. 128, 1197 – 1204, 2008.*
8. *Liang, L.; Xu, Y.; Wu, D.; Sun, Y. A Simple sol-gel route to ZrO_2 films with high optical performances. Mater. Chem. Phys. 114, 252 – 256, 2009.*
9. *K. Anandhan and V. Rajendran, Journal of physical sciences. **17**, 179, ISSN: 0972-8791, 2013.*
10. *A.Tokeer Ahmad, S.Mohd Shazad, P.Rubi Phul, Material Sci & Eng Int J **3** ,100, DOI 10.15406/mseij.2017. 01.00017, 2017.*
11. *J.Tian et.al., Small, **9**, 3864, 2013.*
12. *H.Eskandarloo et.al., Ind. Eng. Chem. Res. **53**, 6881, 2014.*
13. *G.Feng et.al., J.phy.chem.B, **108**, 8119, 2004. Y. Wang et.al., RSC Adv., **8**, 6752, 2018.*
14. *B. Neppolian et.al., Synthesis and characterization of ZrO_2 - TiO_2 binary oxide semiconductor nanoparticles: Application and interparticle elctron transfer process, appl. Catal. A, **333**, 264, 2007.*
15. *L.J. Lai and C.S.Su. Lumineseence excitation and near edge x-ray absorption spectra of Er_2 O_3 dopant on zirconia ceramics, Mater. Chem. Phys., **62**, 148, 2000.*
16. *M.N. Tahir et.al., Facli synthesis and characterization of mono crystyline cubic ZrO2 nanoparticles, solid state sci., **9**, 1105, 2007.*
17. *J. JoO et.al., Multigrm scale synthesis and characterization of monodisperse tetragonal zirconia nanocrystal, J.Am.chem.soc.,**125**, 6555, 2003.*
18. *S. Rasalingam et.al., Applied Catalysis B: Environmental, **148**, 394, 2014.*
19. *V.L.Chandraboss et.al., Mater. Res. Bull., **48**, 3707, 2013.*
20. *S.Balachandran et.al., RSC Adv., **4**, 4353, 2014.*
21. *J. Kamalakkannan et.al., RSC Adv., **5**, 77000, 2015.*
22. *V.L.Chandraboss et.al., RSC Adv., **5**, 25857, 2015.*
23. *K.Ameta et.al., Rev. Chem. Commun. **4**, 38, 2014.*
24. *B.Subash et.al., M, Sep. Purif. Technol. **96**, 204, 2012.*
25. *S. Balachandran et.al., RSC Adv., xx, **1**, 1, 2014.*
26. *J. Lukac et.al., Appl. Catal. B, **74**, 83, 2007.*
27. *Y.M. Wang et.al., J. Mol. Catal. A, **215**,137, 2004.*
28. *S. Singaravelu, G. Balasubramanian, (IJRTE) **2**, 2277, March 2013*
29. *A. Mohamed Ibraheem, J. Kamalakkannan, Materials Science for Energy Technologies, **3**, 183, 2020.*
30. *K. Sharma et.al., Nanoscale Research Letters, **13**,38 1https://doi.org/10.1186/s11671-018-2760-6, 2018.*